JOURNAL OF THE KOREAN ASTRONOMICAL SOCIETY
43: 65 ~ 74, 2010 June

THE ATMOSPHERE PARAMETERS AND THE LINE PROFILE VARIATIONS OF ρ PUPPIS

A.V. YUSHCHENKO[1], T.N. DOROKHOVA[1], V.F. GOPKA[1], CHULHEE KIM[2], B.-C. LEE[3], V.A. YUSHCHENKO[4], AND D.N. DOIKOV[5]

[1]Odessa Astronomical Observatory, Odessa National University, Park Shevchenko, Odessa, 65014, Ukraine
E-mail : avyushchenko@gmail.com, gopkavera@mail.ru

[2]Division of Science Education, Institute of Fusion Science, Chonbuk National University, Chonju 561-756, Korea
E-mail : ckim@chonbuk.ac.kr

[3]Korea Astronomy and Space Science Institute, 61-1, Whaam-Dong, Youseong-Gu, Daejeon 305-348, Korea
E-mail : bclee@boao.re.kr

[4] Dep. of Astronomy, Odessa National University, Park Shevchenko, Odessa, 65014, Ukraine

[5] Dep. of Common Science, Odessa National Maritime University, 65029, Odessa, Ukraine
E-mail : doykovdmitr@mail.ru

(Received April 19, 2010; Accepted May 20, 2010)

ABSTRACT

We investigate ρ Pup using the high resolution spectral observations taken from the VLT archive and observations at a 1.8m–Korean telescope with BOES spectrograph. The atmospheric parameters are determined using the iron–line abundance analysis. We derive an effective temperature value of $T_{\rm eff}$=6890±250K, surface gravity of $\log g$=3.28±0.3 dex, microturbulent velocity of $v_{\rm micro}$=4.1±0.4 km s^{-1}, and the iron abundance of log N=7.82±0.15. The projected rotational velocity of the star is close to $v \sin i$ =3.5 km s^{-1}. Asymmetric line profiles in the observed spectra and variation of this asymmetry with time show that both strong radial pulsation and weak non-radial pulsations are present in ρ Pup.

Key words : stars: oscillation – stars: variables (ρ Pup) – stars: individual (ρ Pup)

1. INTRODUCTION

ρ Pup (HR 3185, HD 67523) is a prototype of the group of metallic-line pulsating variables as well as the well-known δ Del (see Rodriguez & Breger 2001 for a definition). The main period (P=0$^{\rm d}$.14) of the almost sinusoidal light curve of ρ Pup is stable within $\pm 8 \cdot 10^{-8}$ per year (Moon & van Antverpen 2009). The amplitude of brightness variations (near 0.1 mag) seems to be constant (Eggen 1956; Baglin et al. 1973; Kurtz 1976).

The main pulsation was generally agreed to be radial (Campos & Smith 1980; Dall & Frandsen 2002 and references therein). Yang et al. (1987), on the basis of precise differential radial velocities of ρ Pup with a time resolution of less than P/15, determined the precise 2K amplitudes for Ca II, H I, Fe I, Si I, and S I. The results of this investigation support that the 2K value of ρ Pup (93 km s^{-1} per mag) is typical for radial pulsators.

From radial velocity variations , based on observations obtained with 1.4 m CAT telescope at ESO (La Silla, Chele) with spectral resolving power $\Delta\lambda/\lambda$ around 60,000, Mathias et al. (1997) found evidence for two additional, possible secondary, non-radial pulsations (NRP) at frequencies of 7.8 c/d and 6.3 c/d but at a very low level.

A preliminary result reported by Antoci et al. (2008), based on 1200 high resolution high S/N spectra obtained at UCLES spectrograph of the AAT telescope and HARPS spectrograph of the 3.6 meter ESO telescope, shows only the main frequency. Antoci et al. (2009), using additional spectral observations at the 1.2 meter Swiss Leonard Euler telescope and 30 days of photometry with MOST satellite, recently published a short overview of the discovery of at least two frequencies, attributed to NRP.

Antoci et al. (2008, 2009) reported a projected rotational velocity $v \sin i$ of 14.0±1.5 km s^{-1}. This result is close to the first determination of 16 km s^{-1} (Oke & Greenstein 1954) and all later measurements.

In the first detailed investigation of ρ Pup, Greenstein (1948) reported enhanced abundances of iron and heavier elements up to gadolinium. The abundance pattern of ρ Pup was a subject of papers by Bessell (1969), Breger (1970), and Kurtz (1976). Burkhart & Coupry (1991) first investigated the chemical composition of ρ Pup after the end of the photographic era. The abundances of Li, Al, Si, and Fe were investigated. Hui-Bon-Hoa (2000) found the abundances of Mg, Ca,

Corresponding Author: Chulhee Kim
T.N. Dorokhova died in August, 2009

Sc, Cr, Fe, and Ni. Burkhart et al. (2005) published the abundances of Li, Al, Si, S, Fe, Ni, and Eu.

ρ Pup was one of the key objects of the discussion initiated by Kurtz (1976) on metallicism and pulsation. This discussion (see for the details Kurtz et al. 1995; Kurtz 1998; Kurtz 2000), led to the discovery and investigation of some marginal and classical Am-pulsators. Some aspects of the diffusion theory were corrected, and, on the basis of a new model, it was shown that the low amplitude pulsation could be exited in marginal Am stars, and that the evolved Am stars are expected to be variable in the red part of the instability strip (Turcotte et al. 2000).

Dispite the extensive study, no careful investigations of the chemical composition of ρ Pup have been published with high signal to noise receivers. To achieve our aim of the detailed abundance pattern of ρ Pup, it is necessary to acquire values of the effective temperature, surface gravity, and iron abundance. In the third section of the paper we determine these parameters and discuss the possible errors.

The second paper of this short series will be devoted to the chemical composition of ρ Pup. The spectrum synthesis method will be used to reduce the scatter and increase the number of investigated chemical elements. In this method, a theoretical spectrum is fit to the observed spectrum which necessitates a realistic approximation of line profiles. The projected rotational velocity and other possible mechanisms of the broadening of spectral lines need to be investigated.

In the fourth section of this paper we restrict ourselves to the construction of a simple model to describe the line profile at the moment of obtaining of the used VLT spectrum. This model should be sufficient for the investigation of the chemical composition. Unfortunately, our short observational run is not sufficient to create a better model where the variability of line profiles is considered.

The full description of line profiles, especially the variation of profiles with time needs additional observation, and at least several pulsation cycles should be covered.

2. OBSERVATION AND DATA REDUCTION

The spectra of ρ Pup from the VLT archive (Bagnulo et al. 2003) were used. The spectral resolving power of these spectra is R=80,000, the S/N ratio is greater than 300 in the red spectral region, and the wavelength coverage is 3040–5770, 5840–8540, 8662–9182, 9184–9321, 9325–9465, 9470–9612, 9620–9765, 9775–9922, 9933–10085, 10093–10253, and 10258–10400 ÅÅ. All spectra were obtained from JD 2452237.37322 to JD 2452237.377 which is less than 0.03 phase interval of the main pulsational period.

The spectra were taken from the ESO site in the form of wavelength-intensity tables. The latest version of URAN software (Yushchenko 1998) was used for all the next steps of data processing, including the placement of continuum, measurement of equivalent widths, and fitting of observed spectrum by synthetic ones.

Table 1.
Heliocentric radial-velocities for the Hα line.

HJD-2454846	V_r (km s^{-1})
0.1438	52.45
0.1477	52.71
0.1516	53.01
0.1555	52.95
0.1593	52.85
0.1632	52.36
0.1671	52.20
0.1710	51.83
0.1748	51.09
0.1788	50.18
0.1826	49.22
0.1865	48.49
0.1904	47.51
0.1943	46.63
0.1982	45.61
0.2020	44.97
0.2059	44.41
0.2098	43.90
0.2137	43.53
0.2175	43.39
0.2216	43.45
0.2254	43.26

To check the variability of the line profiles we obtained 22 spectra of ρ Pup using the fiber echelle spectrograph BOES * fed by the 1.8-meter telescope of Bohyunsan Optical Astronomy Observatory (BOAO) in Korea. The spectra were recorded from JD2454846.1438 to JD 2454846.2254. The exposure time was five minutes, spectral resolving power R=90,000, S/N=100 in the red spectral region, and wavelength coverage from 3800 to 8870 Å. As a southern object, ρ Pup is too low on the horizon in Korea, with observations only being possible during two hours near the culmination. The BOES spectra were reduced using the IRAF (Tody 1986) code. Table 1 shows the Julian dates of observations and radial velocities of the Hα line obtained using the bisectors of this line.

3. DETERMINATION OF ATMOSPHERIC PARAMETERS AND METALLICITY FROM SPECTRAL OBSERVATIONS

Greenstein (1948) determined the surface gravity for ρ Pup of $\log g$=2.5, compared to Danziger & Dickens (1967)'s value of $\log g$=2.2. Bessel (1967, 1969) used

*A detailed description of the spectrograph is given at http://www.boao.re.kr/BOES/

significantly higher surface gravity values of $\log g$=3.4 and $\log g$=3.2, and a value of $T_{\rm eff}$=6800 K. Breger (1970) reported a value of $T_{\rm eff}$=7000 K, and surface gravity of $\log g$=3.3. Kurtz (1976)'s paper gives $T_{\rm eff}$=7100 K, and $\log g$=3.25. Hui-Bon-Hoa (2000) reported $T_{\rm eff}$=6920 K, and surface gravity $\log g$=3.7.

A similar set of parameters was derived by Burkhart et al. (2005): $T_{\rm eff}$=6920 K, $\log g$=3.70, $v_{\rm micro}$=4.1 km s^{-1}, [Fe/H]=+0.39. Ramirez & Melendez (2005) reported $T_{\rm eff}$=6710±82 K. Netopil et al. (2008) found $T_{\rm eff}$=6820±70 Kusing $uvby\beta$, Geneva, and UBV photometric calibrations. Cenarro et al. (2007) used the values $T_{\rm eff}$=7010 K, $\log g$=3.15, [Fe/H]=+0.34 on the basis of a critical compilation of previous investigations. Antoci et al. (2008, 2009) used the values $T_{\rm eff}$=6900±150 K, and $\log g$=3.80±0.2, obtained from high resolution spectral observations. Using Kunzli et al. (1997)'s calibration of Geneva photometry, we found $T_{\rm eff}$=6649±43 K, $\log g$=3.22±0.15, and [Fe/H]=+0.40±0.06.

Gopka et al. (2007) used the atmospheric parameters $T_{\rm eff}$=7000 K, $\log g$=3.50, and $v_{\rm micro}$=3.8 km s^{-1} to find the first iteration for the abundances of chemical elements in the atmosphere of ρ Pup. Gopka et al. (2007)'s parameters were used to calculate the synthetic spectrum for the whole observed wavelength range. We used Kurucz (1993)'s SYNTHE code, line data were taken from Kurucz (1993, 1995)'s data base, Hirata & Horaguchi (1995)'s line list, Morton (2000)'s, DREAM database (Biemont et al. 2002), the VALD database (Piskunov et al. 1995), Fuhr & Wiese (2006), and other sources.

A synthetic spectrum helps to place the continuum level and to identify the unblended lines of 131 lines of neutral iron and 50 lines of ionized iron so that they can be used to determine more reliable values of afore mentioned atmospheric parameters directly from the observed spectrum.

The profiles of all the lines in the observed VLT spectra show detectable asymmetry, which will be discussed in the next section. Using the calculations of the synthetic spectrum, we selected the best 34 clean lines of neutral iron with a wavelength longer than 5900 Å. These lines are marked in Table 2. The same list of 34 lines was also used to construct the LSD profile, as it will be described in the next section.

We found that the equivalent widths measured using only the blue wings of the line profiles of the clean lines of neutral iron exceed the values found from the opposite wings of these lines by 1.114±0.028. This relation was used to estimate the equivalent widths of iron lines with only one clean wing.

To determine the atmospheric parameters we used the method developed by Yushchenko et al. (1999), which has been described in more detail by Gopka et al. (2004). It was applied in our recent investigations of stars of different types. Briefly, the iron abundances are found for a grid of atmosphere models with different values of temperature, surface gravity and microturbulent velocity. For all models, the correlations between the abundances of iron derived from the individual iron lines, the equivalent widths and the energies of the low level of these lines were calculated.

For part of the lines, we calculated the solar oscillator strengths using the Liege Solar Atlas (Delbouille et al. 1973) and Grevesse & Sauval (1999)'s solar model.

Table 2 (The full table is available in the electronic version of this paper) contains the list of iron lines measured in the VLT spectrum of ρ Pup. Figs. 2, 3 and 4 show the dependencies of calculated abundances vs. equivalent widths, low level energies and wavelengths for the lines of neutral iron. For most of the lines, the oscillator strengths from Fuhr & Wiese (2006) were used.

The analysis of abundance calculations for a grid of atmosphere models permits to select the best parameters. The results of the last iteration are shown in Fig. 1.

The true values of effective temperature and surface gravity should be inside the region of intersections of the dark edges in panel F of this figure: the $T_{\rm eff}$ values range from 6700 K to 7080 K, the surface gravities from $\log g$=2.90 to $\log g$=3.5.

We selected the following values inside this region: $T_{\rm eff}$=6890 K, and $\log g$=3.28. The best microturbulent velocity for this model is $v_{\rm micro}$=4.1 km s^{-1}, and the iron abundance calculated using 131 lines of neutral iron is log N(Fe)=7.82±0.07 (in the scale log N(H)=12). The abundance of iron obtained from only 34 best lines of neutral iron is log N(Fe)=7.82±0.06. Fifty lines of ionized iron give the abundance of log N(Fe) =7.84±0.05. As shown in Fig. 1, several criteria are available to select the values of effective temperature and the surface gravity. The use of several criteria permits more reliable determination of the atmospheric parameters.

Fig. 1, especially panel F presents a clear picture of the possible errors introduced in the determination of the effective temperature and the surface gravity of ρ Pup. These are the internal errors of the used method. The uncertainties are increased by systematic errors arising from the calibration of the scale of effective temperatures, the measurements of equivalent widths, the placement of the continuum level, the atmosphere models, the oscillator strengths, the non-LTE effects and other reasons. Therefore, accepting and including these possible systematic errors, we assigned realistic values of effective temperature, surface gravity, microturbulent velocity, and metallicity as 250 K, 0.3 dex, 0.4 km s^{-1}, and 0.15 dex, respectively.

There are no large discrepancies between the effective temperature values of ρ Pup obtained by different investigators. The mean value of the temperatures of ρ Pup, cited above of $T_{\rm eff}$=6893±130 K exactly coinsides with our determination of $T_{\rm eff}$=6890 K.

The determinations of the surface gravity show large

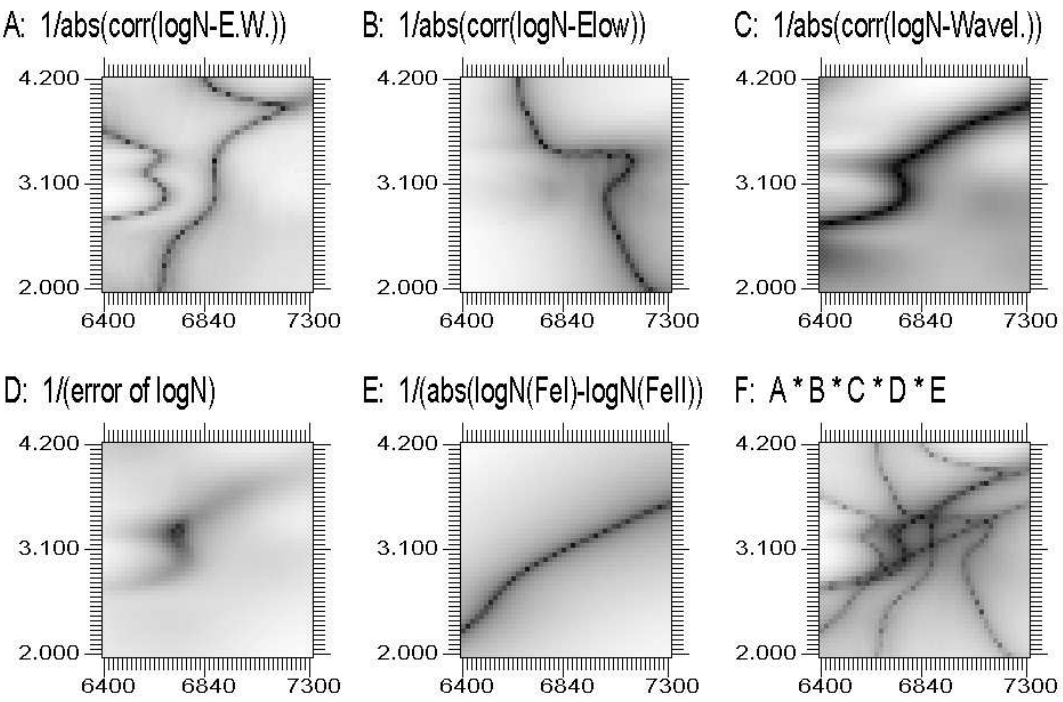

Fig. 1.— Determination of atmospheric parameters of ρ Pup. The panels A-C show the correlation coefficients between the iron abundances found from individual lines of neutral iron and the equivalent widths, the energies of low level, and the wavelengths of these lines respectively. The darkness of the panels is proportional to the reciprocal values of the correlation coefficients. Panel D displays the reciprocal values of errors of mean iron abundance, calculated using the lines of neutral iron. Panel D – the reciprocal values of differences between the iron abundances found using the lines of neutral and ionized iron. Panel F is the multiplication of panels A-E. The axes of each panel are the effective temperatures and the logarithms of surface gravities. Kurucz (1995)'s grid of atmosphere models with metallicity [Fe/H]=+0.3 was used for these calculations.

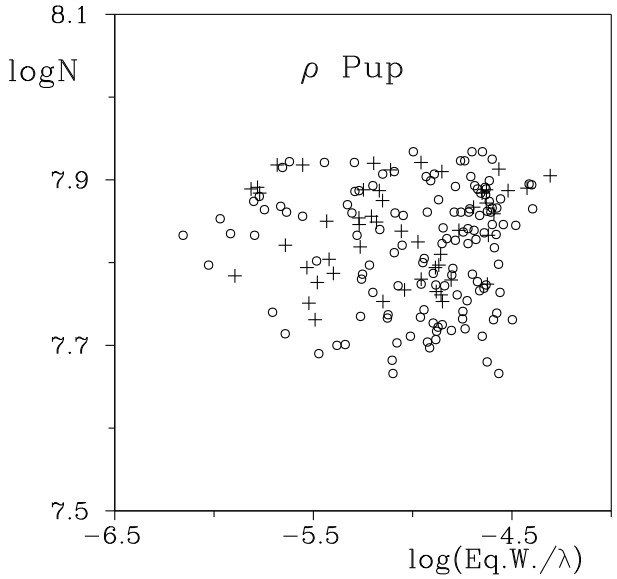

Fig. 2.— The dependence of iron abundances derived from the lines of neutral iron (circles) and ionized iron (crosses) in the spectrum of ρ Pup vs. the equivalent widths (log(W/λ) of these lines.

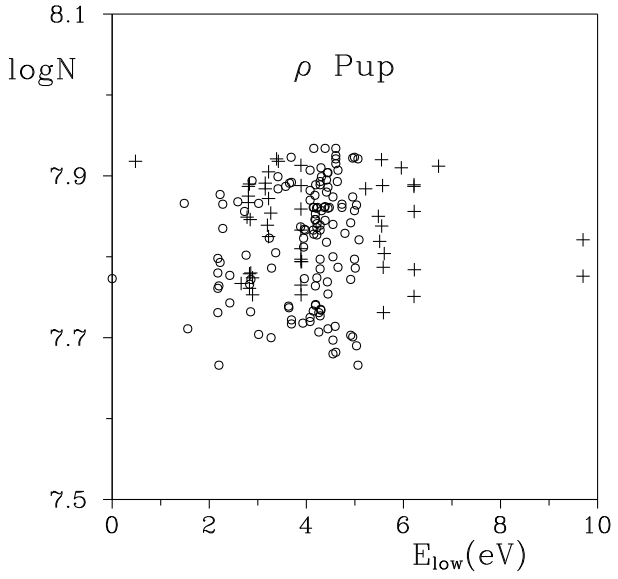

Fig. 3.— The dependence of iron abundances derived from the lines of neutral iron (circles) and ionized iron (crosses) in the spectrum of ρ Pup vs. the energies of low level of these lines.

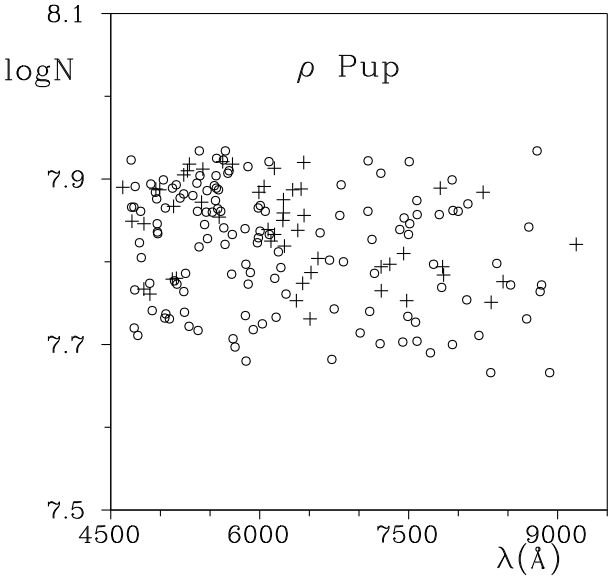

Fig. 4.— Similar to Figs. 1 and 2, but the argument is the wavelength.

scatter. If we omit the outliers with values less than $\log g$=3, the mean surface gravity is $\log g$=3.42±0.23. Netopil et al. (2008) discussed the problems of using the photometrical calibrations of temperature for peculiar stars. The problems of surface gravity calibrations seem to be more complicated. Hui-Bon-Hoa (2000) and Burkhart et al. (2005) found $\log g$=3.7 from $uvby\beta$ photometry, Antoci et al. (2008) derived $\log g$=3.8 using only 8 lines of ionized iron, We hope that the direct determinations of surface gravities of metallic line stars from high resolution spectroscopy contain smaller systematic errors than the photometric calibrations. Our value of surface gravity confirms the earlier values of Bessel (1967, 1969) and Breger (1970) derived from spectral observations.

It should be noted that the main sources of scatter (±0.12 dex) in Figs. 2-4 are the oscillator strengths of the used lines, the uncertainties of atmosphere models, and the contamination of used line widths by the lines of other chemical elements. Even in the investigations of highest quality spectra, for example the Solar spectrum (Grevesse & Sauval, 1997), the scatter is ±0.10 dex.

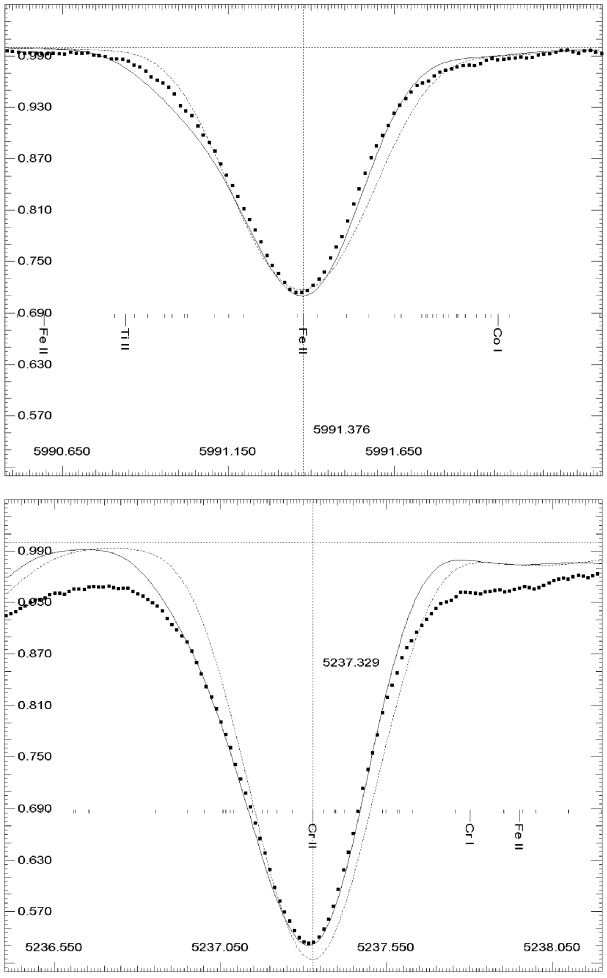

Fig. 5.— The observed (points) and synthetic (solid and dotted lines) spectra of ρ Pup in the vicinities of the Fe II λ 5991.376 Å (upper panel) and Cr II λ 5237.329 Å (lower panel) lines. The axes are the wavelength in angstroms and relative fluxes. The positions of the spectral lines taken into account in the calculations are marked in the bottom part of the figure. Identifications for the strongest lines are given. The positions of the Fe II λ 5991.376 Å and Cr II λ 5237.329 Å lines is marked by a vertical dotted lines. Solid line is the synthetic spectrum convoluted with parameters l=3, m=1, pulsation amplitude 15 km s^{-1}, $v \sin i$ =3.5 km s^{-1}, and instrumental profile R=80,000. Dotted line - synthetic spectrum convoluted with $v \sin i$ =15.3 km s^{-1}, instrumental profile R=80,000.

4. LINE PROFILES

As noted in the previous section, all line profiles in the VLT spectra of ρ Pup are not symmetric. The disturbance of the profiles is similar for all lines. We build a simple model to fit the observed line profile with the calculated one. This model should be sufficient to determine the chemical composition using the spectrum synthesis method. As all the lines in the observed spectrum are disturbed in a similar way, it is possible to propose any of a number of numerical tricks to fit the profiles. It can be the use of a disturbed Voigt profile, the use of a Fourier or power series, or combining the spectrum of a faint secondary component with the same temperature and gravity. It will be possible to fit the observed spectrum, but none of these tricks has any physical sense.

Table 2.
Abundances of iron in the atmosphere of ρ Pup. Individual lines.

	λ (Å)	log gf	E_{low} (eV)	Eq. width (mÅ)	log N (log N(H)=12)
Fe I	4704.948	-1.57^K	3.686	82	7.923
Fe I	4710.284	-1.61^F	3.017	125	7.866
Fe I	4733.591	-2.99^F	1.485	119	7.866
...	...	...	...	...	...

Remarks: K - Kurucz (1993, 1995) oscillator strengths,
S - solar value of oscillator strengths,
F - oscillator strengths are taken from Fuhr & Wiese (2006),
V - oscillator strengths are taken from VALD database,
L - line was used to construct the LSD profile.

A full investigation of the line profiles and their variation with time is beyond the scope of this paper. To achieve this aim it is necessary to obtain high resolution spectra at least for several pulsational cycles, as already done by Antoci et al. (2008, 2009).

Our intention is to construct a very simple model based on physical phenomena, rather than on numerical tricks. Of course not all the model parameters will be confirmed in later publications, but we hope nevertheless that such a model will enable us to use spectrum synthesis for abundance determinations, and that at least some of the parameters of the model will reflect the physical reality.

The most important reasons of asymmetry may be granulation and non-radial pulsations (see, for example, Aerts et al. 1992; Aerts 1996).

Granulation is important in atmospheres with convection, such as in Procyon, which is only slightly cooler than ρ Pup (Gray 2009). Granulation can produce the asymmetry of the lines which is comparable with the asymmetry, detected in the VLT spectra of ρ Pup. If this asymmetry is due to granulation, usually the profiles should not vary with time. The upper and lower parts of line bisector are usually shifted to the red with respect to the middle part of bisector, blue shifts are rare but also possible (Gray 2009). The typical values of these shifts is of the order of several hundreds meters per second in the solar spectrum.

The chemical composition of ρ Pup proves that the star has a radiative atmosphere. Usually the phenomenon of metallic line stars is explained by atomic diffusion (Michaud 1970; Michaud et al. 2008). This effect is effective in radiative atmospheres, where it is suppressed by convection. The investigations of the chemical composition of ρ Pup cited in the first section of this paper revealed it to be a metallic line star, which suggests that atomic diffusion should work effectively in its atmosphere.

Granulation should not play an important role in peculiar stars of the upper main sequence. As is shown below, the line profiles in the spectrum of ρ Pup are variable. These two reasons permit us to conclude that granulation cannot be the main reason for the disturbance of line profiles.

But the effective temperature of ρ Pup is close to the temperatures of stars with convective atmospheres with known granulation effects. Therefore, the possible existence of granulation cannot be excluded. NRP is another possible reason for the asymmetry of line profiles.

Yushchenko et al. (2005) found that the lines in the spectrum of δ Sct are disturbed by NRP. The main frequency of pulsation in the atmosphere of ρ Pup is a radial one, but Mathias et al. (1997) and Antoci et al. (2009) found a weak NRP in this star.

In Section 4.1, we build a model of NRP which fits the used VLT spectra of ρ Pup, but only these spectra. Section 4.2 shows that the high value of the projected rotational velocity used in previous investigations of ρ Pup is incompatible with the observed high resolution spectra. Section 4.3 shows the variations of line profiles with time.

4.1 Asymmetry of Line Profiles and NRP

We presume that the asymmetry of line profiles can be explained by NRP and try to find the combination of modes capable of fitting the line profiles in the VLT spectra. We do not try to describe the variability of line profiles.

The above mentioned list of 34 clean iron lines was used to construct the mean line profile in the spectrum of ρ Pup using the LSD method described by Reiners & Royer (2004). The LSD profile was used as a mean observed profile. We fit the LSD profile by the synthetic spectrum disturbed by NRP.

We developed URAN software (Yushchenko 1998) to integrate the flux from the disk of a nonradially pulsating star. The disk of the star was divided into several thousand regions. For each of these regions the synthetic spectrum was calculated using Kurucz (1993) SYNTHE code. The velocity shift for each region was calculated as the sum of the NRP and rotation of the star. The number of regions, the combination of NRP

modes, and the projected rotational velocity were selected to adjust the observed LSD profile. We took into account only the velocity fluctuations. Integration over the stellar disk resulted in a synthetic profile influenced by NRP and rotation. Test calculations show the possibility to reproduce Berdyugina et al. (2003)'s results.

Fig. 5 shows the observed profile of ρ Pup and the synthetic spectrum disturbed by NRP and rotation with the pulsation degree mode of l=3, the azimuthal number of m=1, and the NRP amplitude of 15 km s^{-1}. The synthetic spectrum was additionally broadened by rotation with a projected rotational velocity of $v \sin i$ =3.5 km s^{-1}. The LSD profile was built using the lines of neutral iron, but all lines in the VLT spectra show similar profile disturbances. We select the lines of ionized iron and ionized chromium for Fig. 5 to show that the synthetic profile can fit all lines in the spectrum with sufficient accuracy. Note that Figs. 6 and 7 also show the fit of the observed spectrum by the calculated one.

Our model can fit the observed profiles in the used VLT spectra. These parameters will be used to determine the chemical composition of the atmosphere, although it cannot be confirmed whether these are the real NRP parameters for ρ Pup. Additional observations are necessary to find the true parameters.

4.2 Projected Rotational Velocity

As afore mentioned, the line profiles were broadened with projected rotational velocity of $v \sin i$ =3.5 km s^{-1}. Mathias et al. (1997) found $v \sin i$ =15.3 km s^{-1}, but this value is inconsistent with the high resolution VLT spectra, as shown in Figs. 5, 6 and 7.

Fig. 5 compares the observed spectrum with the synthetic spectra convolved with a high value of projected rotational velocity and with a lower value of $v \sin i$ combined with pulsational broadening of the profile. Note that these lines were not used for the determination of the LSD profile. Analysis of this figure indicates that isolated lines in the red part of the spectrum can be fitted by both sets of broadening parameters with sufficient accuracy, but that the use of the higher projected rotational velocity results in a slightly wider profile and, of course, in the absence of the asymmetry of profiles.

Figs. 6 and 7 show the lines in the blue part of the spectrum, where the blending effects cannot be neglected. This part of the spectrum proves that the isolated lines can be fitted both by $v \sin i$ =15.3 km s^{-1} , and by our model with comparable precision. But the approximation of close pairs of lines and faint lines cannot be achieved with the high value of the projected rotational velocity. The fit of the close pairs is significantly better in the case of the lower value of $v \sin i$ combined with the pulsational broadening of spectral lines.

BOES spectral observations show the similar appearance of the line profiles and are not consistent with either the appearance of the line profiles or with the high value of the projected rotational velocity.

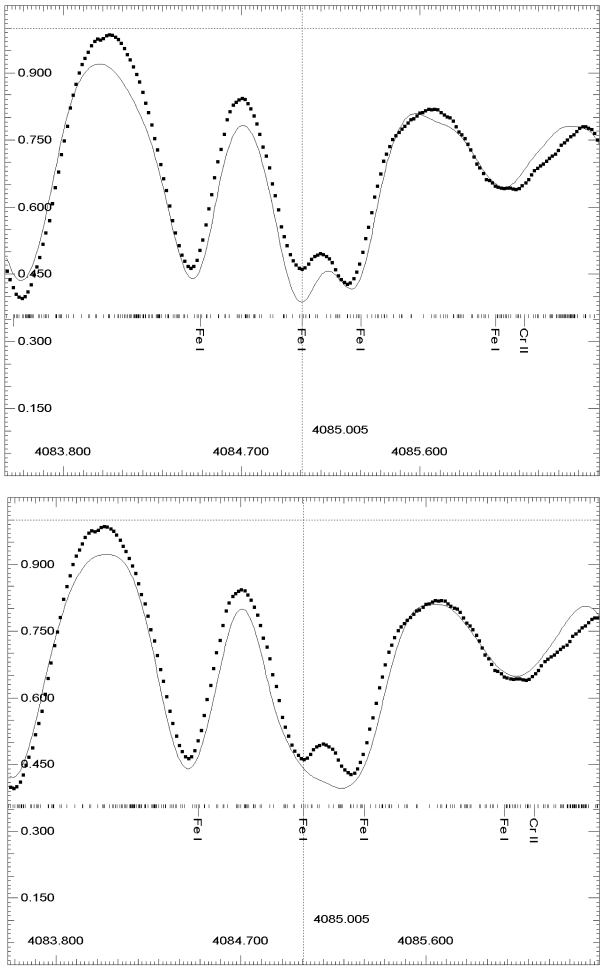

Fig. 6.— The observed (points) and synthetic (lines) spectra of ρ Pup in the vicinity of the Fe I λ 4085.005 Å line. The axes are the wavelength in angstroms and the relative fluxes. The wavelengths of the spectral lines taken into account in the calculations are marked in the bottom part of the figure. Identifications are given for the strongest lines. The position of the Fe I λ 4085.005 Å line is marked by a vertical dotted line. The synthetic spectrum is convoluted with two sets of parameters. Upper panel – l=3, m=1, amplitude of pulsation 15 km s^{-1}, and $v \sin i$ =3.5 km s^{-1}. Bottom panel – zero amplitude of pulsation, $v \sin i$ =15.3 km s^{-1}.

4.3 Variations of Line Profiles

The best way to prove the existence of NRP in ρ Pup is to obtain high resolution time series observations and to determine the modes of these pulsations. We observed 22 spectra of ρ Pup with BOES spectrograph attached to a 1.8-m Korean telescope.

Unfortunately our short time series covers only 0.6

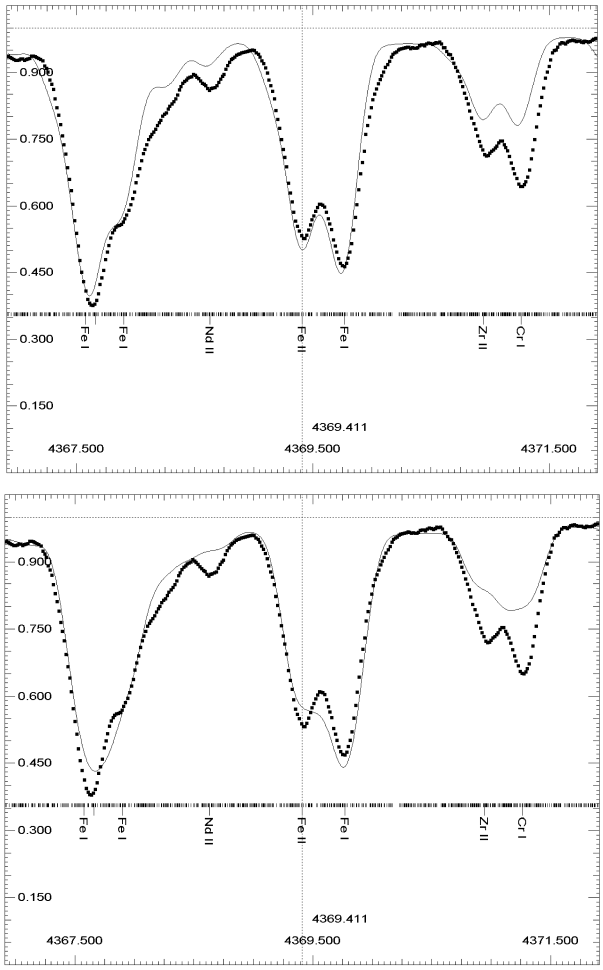

Fig. 7.— The same as Fig. 6 but for the spectral region with three close line pairs : the first the lines of neutral iron λ 4367.678 Å and λ 4367.903 Å, the second the lines of ionized iron λ 4369.411 Å and the line neutral iron λ 4369.771 Å, and the third the lines of ionized zirconium λ 4370.947 Å and of neutral chromium λ 4371.264 Å. Note that the line of ionized neodymium λ 4368.631 Å and other faint lines disappear if the synthetic spectrum is convolved with the high value of projected rotational velocity.

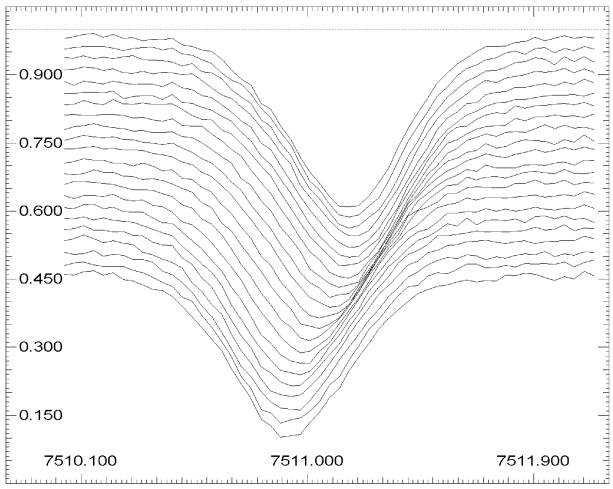

Fig. 8.— 22 BOES spectra of ρ Pup in the vicinity of iron line λ 7511.019 Å. The consequent spectra are shifted by 0.025 in the vertical dimension. The first spectrum is the highest one.

phase interval of the main pulsational period. An attempt to analyze these observations did not produce a quantitative solution. We are unable to point the unique combination of pulsational modes which is responsible for the disturbance of line profiles.

Fig. 8 shows 22 observed spectra of ρ Pup in the vicinity of iron line λ 7511.019 Å. It is evident that the asymmetry of the profile changes with time. To clarify this, Fig. 9 presents the first and last spectra of our short time series near the line of ionized iron λ 5991.376 Å. The bisectors of profiles have different inclination because the asymmetry of the line has been changed. In the first spectrum the red wing of the profile is steeper than the blue one, in the last spectrum the blue wing is steeper. All lines in the spectrum show the similar variations with time. Iron lines λ 7511.019 Å and λ 5991.376 Å were selected for illustration because these lines are located in red spectral region where we can find the isolated lines without strong blending effects.

The variation of the line profiles with time proves that the asymmetry is not due to granulation, but may be a result of NRP. However, only the asymmetry of the line profiles, and no other disturbances of the profiles can be observed.

The stars with stronger NRP show a doubling of line cores and other effects. The phase interval of the main period was observed to be 0.6, but no strong effects were observed. This confirmed, that the radial pulsation is dominant in the atmosphere of ρ Pup, and that NRP is less powerful and results in the asymmetry of profiles only.

5. CONCLUSIONS

The main aim of this paper is to find effective temperature, surface gravity, iron abundance, microturbulent velocity and projected rotational velocities of ρ Pup. Investigation of iron lines in high quality VLT spectra of the star reveals the parameters of its atmosphere. The analysis gives an effective temperature value of $T_{\rm eff}$=6890 K, surface gravity of $\log g$=3.28, microturbulent velocity $v_{\rm micro}$=4.1 km s^{-1}, iron abundance of log N(Fe)=7.82. Using the solar iron abundance of log N(Fe)=7.50 (Asplund et al. 2009), this corresponds to [Fe/H]=+0.32.

The high dispersion spectra of ρ Pup proves that the projected rotational velocity of the star is significantly less than 15 km s^{-1}. Hence the broadening of spectral lines needs to be explained by other phenom-

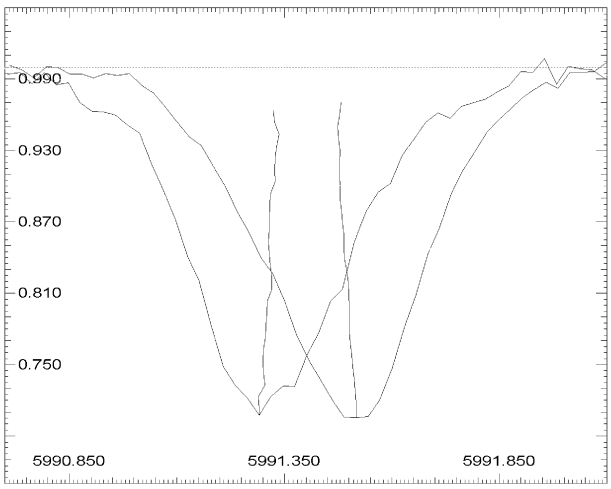

Fig. 9.— The first and the last BOES spectra of ρ Pup in the vicinity of the line of ionized iron λ 5991.376 Å. Bisectors of this line are also shown.

ena. High quality observations reveals the existence of profile variations with time and suggests their physical explanation.

We propose the combination of NRP modes to fit the VLT spectra. This combination will be used in our next paper for spectrum synthesis calculations. We intended to determine the chemical composition of ρ Pup under the assumption of a classical static (non-pulsating) atmosphere. As generally accepted, we use a static atmosphere to investigate a pulsating star. The possible effects of pulsation on chemical composition are relatively small and will be discussed in the next paper.

It should be noted that the used combination of NRP modes cannot describe the spectrum at different phases of pulsation. The self-consistent model of NRP in the atmosphere of ρ Pup needs additional observations. It would be premature to argue that our profile is a unique solution, but it seems sufficient to determine the chemical composition of ρ Pup.

We analyzed 22 high resolution spectra, obtained at a 1.8-meter Korean telescope (these spectra cover a phase interval of only 0.6), and found the variations of profiles of all spectral lines with time. This may have been due to NRP, but the short time series was insufficient to determine the exact modes of the pulsations.

We note that the observations by Antoci et al. (2008, 2009) of several pulsational cycles of this star with high spectral resolution and S/N ratio, can lead to very interesting results.

ACKNOWLEDGMENTS

The present work was possible through the use of data from the UVES Paranal Observatory Project (ESO DDT Program ID 266.D-5655). Also the data from NASA ADS, SIMBAD, and NIST databases were used and we thank the teams and administrators of these projects.

This paper was supported by Korea Science and Engineering Foundation (F01-2006-000-10138-0), and Odessa Astronomical Observatory. Gopka and V.A. Yushchenko were suppported by the Swiss National Science Foundation (SCOPES project No. IZ73Z0 - 128180/1).

REFERENCES

Aerts, C., de Pauw, M., & Waelkens, C. 1992, Mode Identification of Pulsating Stars from Line Profile Variations with the Moment Method. An Example - The Beta Cephei Star Delta Ceti, A&A, 266, 294

Aerts, C. 1996, Mode Identification of Pulsating Stars from Line-Profile Variations with the Moment Method: A More Accurate Discriminant, A&A 314, 115

Antoci, V., Nesvacil, N., & Handler, G. 2008, Rho Puppis: Some Spectroscopic Results or "The Taming of Rho Puppis", Comm. in Astroseimology, 157, 286

Antoci, V., Handler, G., Carrier, F., Grundahl, F., Matthews, J. M., Hareter, M., Kuschnig, R., & Houdec, G. 2009, The Delta Scuti Star Rho Puppis: The Perfect Target to Probe the Theory Predicting Solar-Like Oscillations in Cool Delta Scuti Stars, AIP Conf. Ser. 1170, 440

Asplund, M., Grevesse, N., Sauval, A. J., & Scott, P. 2009, The Chemical Composition of the Sun, Annual Reviews of Astronomy and Astrophysics, 47, 481

Baglin, A., Breger, M., Chevalier, C. et al. 1973, Delta Scuti Stars, A&A, 23, 221

Bagnul, S. et al. 2003, The UVES Paranal Observatory Project: A Library of High-Resolution Spectra of Stars across the Hertzsprung-Russell Diagram, Messenger, 114, 10

Berdyugina, S. V., Telting, J. H., & Korhonen, H. 2003, Surface Imaging of Stellar Non-Radial Pulsations. I. Inversions of Simulated Data, A&A, 406, 273

Bessell, M. S. 1967, A Different Interpretation of rho Puppis, ApJ, 149, L67

Bessell, M. S. 1969, An Investigation of Short-Period Variable Stars. I. The Delta Scuti Stars, ApJS, 18, 167

Biemont, J., Palmeri, P., & Quinet, P. 2002, Database of Rare Earths At Mons University http://www.umh.ac.be/ãstro/dream.html

Breger, M. 1970, An Investigation of Short-Period Variable Stars. I. The Delta Scuti Stars, ApJ, 162, 597

Burkhart, C., & Coupry, F. M. 1991, The A and Am-Fm Stars. I - The Abundances of Li, Al, Si, and Fe, A&A, 249, 205

Burkhart, C., Coupry, F. M., Faraqqiana, R., & Gerbaldi, M. 2005, The field Am and PuppisLike Stars: Lithium and Heavier Elements, A&A, 429, 1043

Campos, A. J., & Smith, M. A. 1980, Pulsational Mode-Typing in Line Profile Variables. II - rho Puppis and Delta Scuti, ApJ, 238, 667

Cenarro, A. J., Peletier, R. F., Snchez-Blquez, P., Selam, S. O., Toloba, E., Cardiel, N., Falcon-Barroso, J., Gorgas, J., Jimenez-Vicente, J., & Vazdekis, A. 2007, Medium-Resolution Isaac Newton Telescope Library of Empirical Spectra –II. The Stellar Atmospheric Parameters, MNRAS, 374, 664

Cousins, A. W. J. 1951, Bright Variables Stars in the Southern Hemisphere, Monthly Notes of the Astronomical Society of South Africa, 10, 60

Dall, T. H., & Frandsen, S. 2002, Mode Characterisation in Delta Scuti Stars. I. rho Pup, GN And, V1208 Aql and AV Cet, A&A, 386, 964

Danziger, I. J., & Dickens, R. J. 1967, Spectrophotometry of New Short-Period Variable Stars, ApJ, 149, 55

Dellbouille, L., Rolland, G., & Neven, L. 1973, Photometric Atlas of the Solar Spectrum from λ 3000 to λ 10000, (Institute de Astrophisique de Universitete de Liège).

Fuhr, J. R., & Wiese, W. L. 2006, New Critical Compilations of Atomic Transition Probabilities for Neutral and Singly Ionized Carbon, Nitrogen, and Iron, J. Phys. Chem. Ref. Data, 35, 1669

Gopka, V., Yushchenko, A., Kim, C., Lambert, D., Rostopchin, S., Kim, S.-L., Jeon, Y.-B., Dorokhova, T., Tarasov, A., & Chernysheva, I. 2007, Chemical Composition of Several Pulsating Variable Stars of the Boo and Sct Types, ASP Conf. Ser., 362, 249

Gopka, V. F., Yushchenko, A. V., Mishenina, T. V., Kim, C., Musaev, F. A., & Bondar, A. V. 2004, Atmospheric Chemical Composition of the Halo Star HD 221170 from a Synthetic-Spectrum Analysis, Astronomy Reports, 48, 577

Gray, D. F. 2009, The Third Signature of Stellar Granulation, ApJ, 697, 1032

Greenstein, J. L. 1948, Spectrophotometry of the F Stars and of Ursae Majoris. I., ApJ, 107, 151

Grevesse, N., & Sauval, A. J. 1999, The Solar Abundance of Iron and the Photospheric Model, A&A, 347, 348

Hui-Bon-Hua, A. 2000, Metal Abundances of Field A and Am Stars, A&AS, 144, 203

Hirata, R., & Horaguchi, T. 1995, SIMBAD Catalog VI/69

Kunzli, M., North, P., Kurucz, R. L., & Nicolet, B. 1997, A Calibration of Geneva Photometry for B to G Stars in Terms of Teff, log G and [M/H], A&AS, 122, 51

Kurtz, D. W. 1976, Metallicism and Pulsation: An Analysis of the Delta Delphini Stars, ApJS, 32, 651

Kurtz, D. W. 1998, Non-Turbulent Pulsation: Metallicism in Pulsating Stars, ASPC, 135, 420

Kurtz, D. W. 2000, Pulsation of Chemically Peculiar and Pre-Main Sequence Stars in the Scuti Instability Strip, ASPC, 210, 2

Kurtz, D. W., Garrison, R. F., Koen, C. et al. 1995, Metallicism and Pulsation: The Discovery of Large-Amplitude Delta Scuti Pulsation in a High-Metallicity rho Puppis Star, HD 40765, MNRAS, 276, 199

Kurucz, R. L. 1993, CDROMs No. 1-18 (Cambridge, MA, Smithsonian Astrophys. Obs.)

Kurucz, R. L. 1995, CDROM No. 23 (Cambridge, MA, Smithsonian Astrophys. Obs.)

Mathias, P., Gillet, D., Aerts, C., & Breitfellner, M. G. 1997, A Spectroscopic Study of the Delta Scuti Star rho Puppis, A&A, 327, 1077

Michaud, G. 1970, Diffusion Processes in Peculiar A Stars, ApJ, 160, 641

Michaud, G., Richer, J., & Richard, O. 2008, Abundance Anomalies in Horizontal Branch Stars and Atomic Diffusion, ApJ, 675, 1223

Moon, T., & van Antverpen, C. 2009, Period Changes in δ Scuti Stars: ρ Puppis, JAAVSO, 37, 3

Morton, D. C. 2000, Atomic Data for Resonance Absorption Lines. II. Wavelengths Longward of the Lyman Limit for Heavy Elements, ApJS, 130, 403

Netopil, M., Paunzen, E., Maitzen, H. M., North, P., & Hubrig, S. 2008, Chemically Peculiar Stars and Their Temperature Calibration, A&A, 491, 545

Oke, J. B., & Greenstein, J. L. 1954, The Rotational Velocities of - - and G-Type Giant Stars., ApJ, 120, 384

Piskunov, N., Kupka, F., Ryabchikova, T., Weiss, W., & Jeffery, C. 1995, VALD: The Vienna Atomic Line Data Base., A&AS, 112, 525

Ramirez, I., & Melendez, J. 2005, The Effective Temperature Scale of FGK Stars. I. Determination of Temperatures and Angular Diameters with the Infrared Flux Method, ApJ, 626, 446

Reiners, A., & Royer, F. 2004, Altair's Inclination from Line Profile Analysis, A&A, 428, 199

Rodriguez, E., & Breger, M. 2001, Delta Scuti and Related Stars: Analysis of the R00 Catalogue, A&A, 366, 178

Tody, D. 1986, "The IRAF Data Reduction and Analysis System" in Proc. SPIE Instrumentation in Astronomy VI, ed. D.L. Crawford, 627, 733

Turcotte, S., Richer, J., Michaud, G., & Christensen-Dalsgaard, J. 2000, The Effect of Diffusion on Pulsations of Stars on the Upper Main Sequence – Scuti andMetallic A Stars, A&A, 360,603

Venn, K. A., & Lambert, D. L. 2008, ApJ, 677, 572

Yang, S., Walker, G. A. H., & Bennett, P. 1987, The Spectral Variations of the Delta Scuti Star rho Puppis, PASP, 99, 425

Yushchenko, A. V. 1998, URAN: A Software System for the Analysis of Stellar Spectra, Proceedings of the 20th Stellar Conference of the Czech and Slovak Astronomical Institutes, Ed. by J. Dusek (ISBN 80-85882-08-6, Brno), p. 201

Yushchenko, A. V., Gopka, V. F., Khokhlova, V. L., Musaev, F. A., & Bikmaev, I. F. 1999, Astronomy Letters 25, 453

Yushchenko, A., Gopka, V., Kim, C., Musaev, F., Kang, Y. W., Kovtyukh, V., & Soubiran C. 2005, The Chemical Composition of Scuti, MNRAS, 359, 865